



Integrating seismic attributes in the accurate modeling of geological structures and determining the storage of the gas reservoir in Gorgan Plain (North of Iran)

Mehdi Rezvandehy^{a,*}, H. Aghababaei^b, S.H. Tabatabaee Raissi^c

^a Department of Geophysics, Dana Energy Company, Tehran, Iran

^b Faculty of Mining Engineering, Sahand University of Technology, Tabriz, Iran

^c Department of Geophysics, Exploration Directorate, National Iranian Oil Company (N.I.O.C.), Tehran, Iran

ARTICLE INFO

Article history:

Received 15 December 2009

Accepted 23 December 2010

Available online 19 January 2011

Keywords:

Gas reservoir

Seismic attributes

3D seismic

Modeling

Gorgan Plain

ABSTRACT

Three dimensional seismic operation of Gorgan Plain was studied around a well, which is situated in North of Iran following the hitting of a thin overpressure gas layer (thickness of 9.6 m), with the purpose of the accurate modeling of geological structures and determining the approximate gas storages. The geological structures of the reservoir were modeled using the seismic attributes (coherence, instantaneous amplitude and spectral decomposition (FFT)). The obtained results clearly demonstrated the shape and volume of the existing structural traps in the studied area. In order to estimate the thickness of gas layer in the 3D seismic volume and determining the gas storage, the thickness changes based on the seismic amplitudes were used because its thickness was less than the critical resolution thickness for this layer. However, due to its low thickness, the lack of indicator peak in seismic sections and strong faults of area, it was difficult to pursue this layer in the seismic volume and map its exact amplitude. Considering this issue, a new method with integrating of seismic attributes was recommended. First, the instantaneous amplitude attribute of the thin reservoir layer reflector in computed synthetic seismogram were fabricated and then the frequency regarding the highest amount (dominant frequency) was chosen by Fourier Transform. Finally, spectral decomposition (FFT) with the resulting frequency was gained over the cross-section of the layer's instantaneous amplitude attribute in the 3D seismic volume choosing a proper time window. In such a situation, an increase of its thickness was seen as its amplitude increase and the minimum gas storage of this reservoir was calculated using the area of the restricted part of high thickness (over 9.6 m).

© 2011 Elsevier B.V. All rights reserved.

1. Introduction

This article is an example of how to implement and integrate seismic attributes in 3D seismic data (post stack) and one well to determine geological structures (structural traps) and the approximate estimation of the existing gas in a gas reservoir (Gorgan Plain). The attributes used for this purpose include 1. coherence, 2. instantaneous amplitude, and 3. spectral decomposition, Fast Fourier Transform (FFT).

1- coherence attribute is the best determiner of anticline structures, faults, deltas, river channels, dikes and other stratigraphic anomalies (Bahorich and Farmer, 1995; Gersztenkorn et al., 1999; Marfurt et al., 1998). In fact, this method calculates the similarity between the seismic traces. 2- instantaneous amplitude is gained by finding quadrature trace from Hilbert transform of actual trace and the calculation of numerical amount of seismic trace which resulted from these two traces (Taner, 1977) and is directly related to acoustic impedance differences (Taner, 2000) (Fig. 1). 3- spectral decompo-

sition (FFT) is calculated by Fourier Transform of traces from time domain into frequency domain and countering the amplitude magnitudes in concerning frequency bands (Partyka et al., 1999). For instance, the red seismic trace in Fig. 2 changes to a trace with amplitude-frequency functions through Fourier Transforms (from time domain to frequency domain). Then, Fourier Transform all the traces are given in a time window and subsequently the frequency cross-sections of the spectral decomposition attribute is achieved. The results gained from this attribute can be considered in the accurate interpretation of layer thickness, demonstrating thin layers and determining the exact anomalies of the amplitudes (Bahorich et al., 2002; Hall and Trouillot, 2004). Each of these attributes contains a particular function and determination of geological structures and hydrocarbon potentials. Therefore, by integrating these, some significant results could be achieved.

In order to determine the gas storage of the reservoir in 3D seismic volume, a relevant thickness modeling of gas layer is needed. Nevertheless, in conditions where the layer thickness is less than its critical resolution thickness it is impossible to estimate thickness of the layer accurately, because for the reflections from the upper and lower surfaces of the layer form one reflector (Widess, 1973). In this

* Corresponding author. Tel.: +98 9111851411; fax: +98 4123444311.
E-mail address: M_Rezvandehy@sut.ac.ir (M. Rezvandehy).

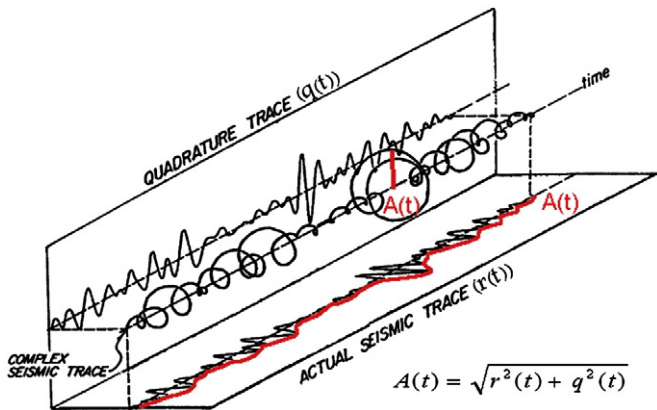


Fig. 1. The method of obtaining the instantaneous amplitude attribute, quadrature trace ($q(t)$) through Hilbert transform of the real seismic trace ($r(t)$) which is later achieved and instantaneous amplitude attribute ($A(t)$) by calculating the numerical amount of the seismic traces is obtained (Taner, 1977).

condition, the increasing model of layer thickness based on seismic amplitude increase should be taken into account (Neidell and Poggiagliolmi, 1977) and so an approximate estimation of layer thickness could be achieved (the increase of the thickness up to tuning thickness is increased and later decreased). For this purpose, the amplitude changes of the reservoir layer can be mapped by following the layer in the 3D seismic volume and calculating the amplitude instantaneously. However, the reservoir layer contains no index peak in its seismic section because of the low thickness and the area is badly filled with faults, therefore it is impossible to follow the layer and map the accurate amplitude magnitudes in the 3D seismic volume with the usual methods. In the present article, a new method of integrating the attributes has been provided.

2. Gorgan Plain

Gorgan Plain is located in north of Iran and south east of the Caspian Sea (Fig. 3). The most important construction in the region called Chelekan, belongs to the Paleocene Period that is mostly formed of green or dark red sand-containing marls together with somehow thick layers of sandstone and conglomerate. This construction is often watery, contains hydrocarbon (mostly gas layers) and is among the inner layer sand masses. Most of the gas collections are inside Chelekan construction and near mud volcano of the region. Most of these mud volcanos have not reached the surface and a few of them like GARNIARIK TEPPE mud volcano have outcrop on the ground. About 10 wells were dug from which the well Go-3 hit an over

pressure gas sand layer near GARNIARIK TEPPE mud volcano and burnt. Thus, the other well Go-3A was dug in a distance 300 m from this well (Fig. 3). This well also hit Chelekan construction. The thickness of this layer was calculated to be 9.6 m with a capacity of 200,000 m³ extractable gas per day. Following this, a 3D seismic operation with the area of nearly 160 km² were carried out around the well Go-3A and GARNIARIK TEPPE mud volcano. The 3D seismic area has 17,575 m length and 8975 m width (number of in line 200 to 560 and cross line 200 to 909) (Fig. 3). In this article, the geological structure modeling of Chelekan construction and the estimation of the minimum extractable gas from well Go-3A is carried out by integrating seismic attributes.

3. Methodology

Before the reservoir has been modeled, it is necessary to model the geological structures particularly structural traps (mud volcano and faults) in the reservoir. Regarding to this purpose, the cross-sectional coherence and five instantaneous amplitude of attribute having vertical cross-sections used on the interpreted structures. In addition, the frequency bands of spectral decomposition attribute were implemented to form and develop it laterally.

In order to estimate the thickness of gas layer in the 3D seismic volume, synthetic seismogram of the well (Go-3A) in this region was built by choosing the best wavelet and having high correlation with seismic data, and the index of critical resolution thickness for the gas layer was calculated. Finally, it was found out that the thickness of this layer is less than the critical resolution thickness. Under such circumstances, thickness changes could be implemented based on seismic amplitudes as a criterion to determine the partial thickness of the gas layer in the 3D seismic volume (Neidell and Poggiagliolmi, 1977). It is impossible to follow the layer and map the accurate amplitude magnitudes in the 3D seismic volume with the usual methods because of the low thickness, the reservoir layer contain any index peak in seismic section, and the area is badly filled with faults.

In terms of mentioned problem, the instantaneous amplitude attribute of the reflector were achieved through the upper and lower surface of synthetic seismogram in the thin reservoir layer. So, the layer mentioned appeared as one peak. Therefore, using Fourier Transform (Bracewell, 1965) of the instantaneous amplitude magnitude, the dominant frequency (frequency of the highest amplitude) of the layer easily achieved. By having the frequency of the instantaneous amplitude peak in the layer, instantaneous amplitude in the 3D seismic volume is first calculated and then output amplitude magnitudes of the spectral decomposition is calculated in terms of prior achieved frequency (Rezvandehy, 2006). Therefore, the accurate changes of the seismic amplitudes in the mentioned layer are achieved in the 3D seismic volume that could be a sign of some partial changes in the thickness (thickness increases with the increase of the amplitude). The instantaneous amplitude was used because this attribute does not depend on seismic phase and is directly related to acoustic impedance differences and negative amounts of seismic traces is omitted. Moreover, the changes of seismic amplitudes are obtained between zero and maximum amounts, so computing dominant frequency for the gas layer would be more straightforward.

4. Modeling of geological structures

4.1. Coherence and instantaneous amplitude attributes

In this region, the upper part of Chelekan construction has more significance than its lower part (Tertiary–Mesozoic unconformity). Therefore, the investigations would be mostly about the upper part of Chelekan construction. Fig. 4 shows the coherence attribute cross-section from Chelekan top in the well Go-3A (time slice 1052 ms). The high coherence is shown in white and the low one is shown in black.

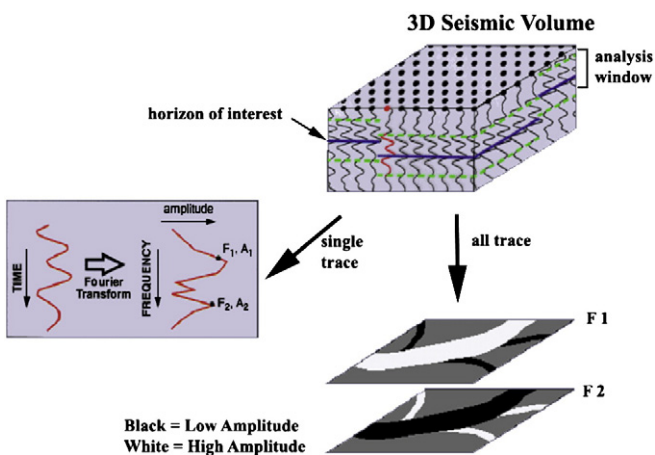


Fig. 2. The method of obtaining spectral decomposition attribute.

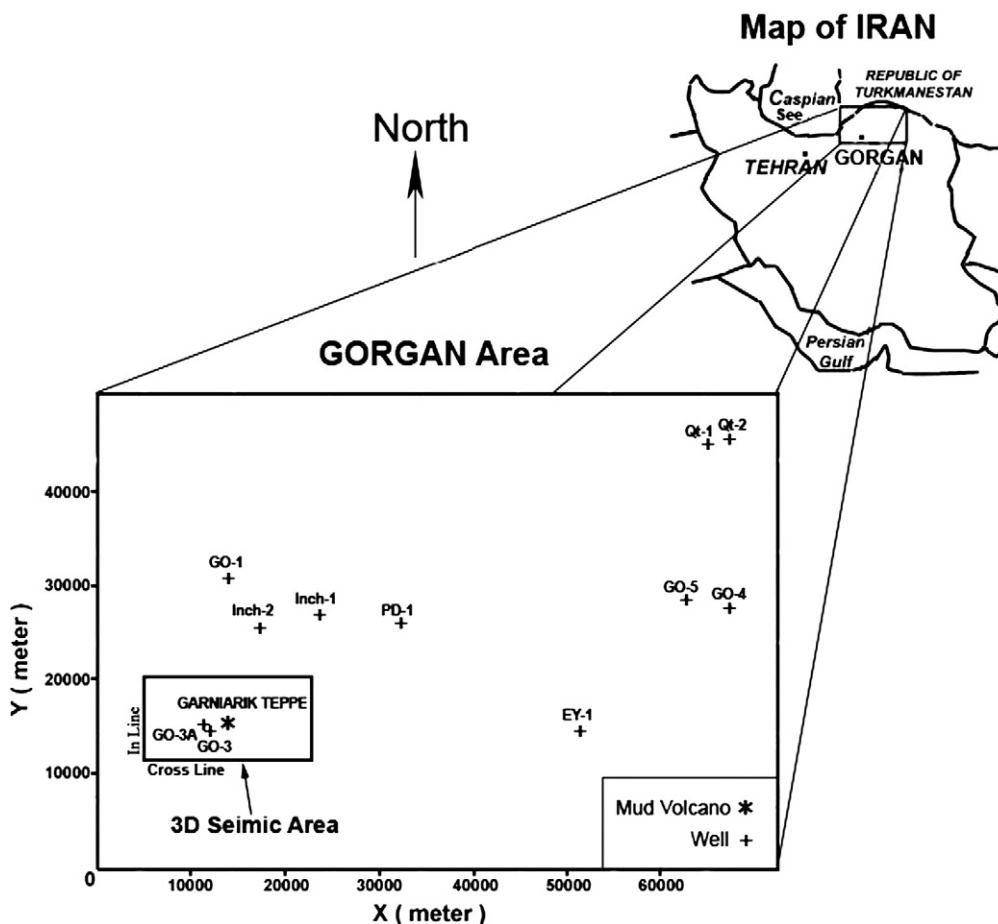


Fig. 3. Location of Gorgan Plain and the wells dug. The three dimensional seismic operations in the region of GARNIARIK TEPPE mud volcano and well Go-3A have been carried out.

Fig. 5 illustrates the vertical cross-sections A-A', B-B', C-C', D-D', and E-E' of the passing instantaneous amplitude attribute from the coherence attribute cross-section (Fig. 4) showing the time line 1052 ms for further approving the structures interpreted from seismic coherence attribute and the time line 1684 ms for subsequent probes of reservoir (Fig. 6). The faults in the coherence cross-section are observed as thin lines of low coherence (black lines), because the fault line indicates the least coherence. In Fig. 4, it is clear that the parallel faults 1 were perpendicular to parallel faults 2 (Rezvandehey, 2006). Therefore, two series of the faults exist in this reservoir. These faults

are also clear in the passing vertical sections (A-A', D-D', and E-E'). Through observing the time slice 1052 ms in Fig. 6 and comparing it with Fig. 4, it was found that the coherence attribute is so effective in indicating geological structures. Most of the faults on time slice cannot be indicated. The instantaneous amplitude attribute also indicates the accurate boundaries of the geological sequences and lateral changes of fault sign. In this vertical cross-section, Chelekan top and Tertiary–Mesozoic unconformity have been determined as having high amplitude that is a result of high acoustic impedance difference in the entering and exiting moment from the watery and sand

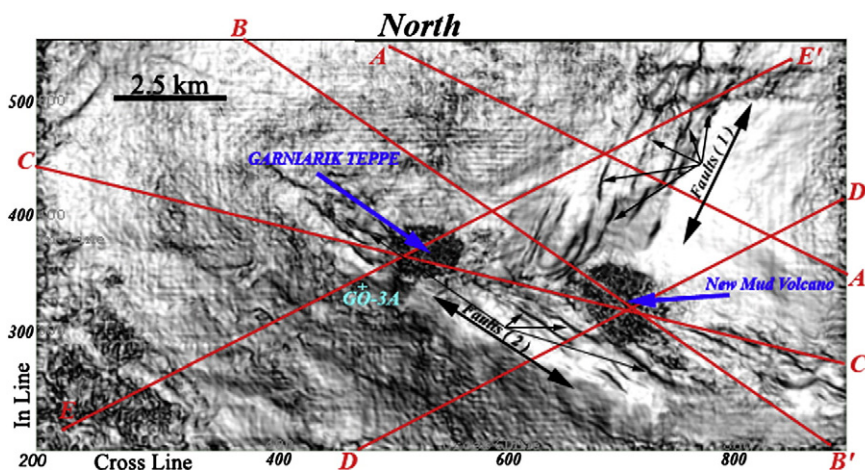


Fig. 4. The horizontal cross-section of coherence attribute in Chelekan top of the well Go-3A (1052 ms) and five vertical cross-section of instantaneous amplitude attribute for accurate interpretation.

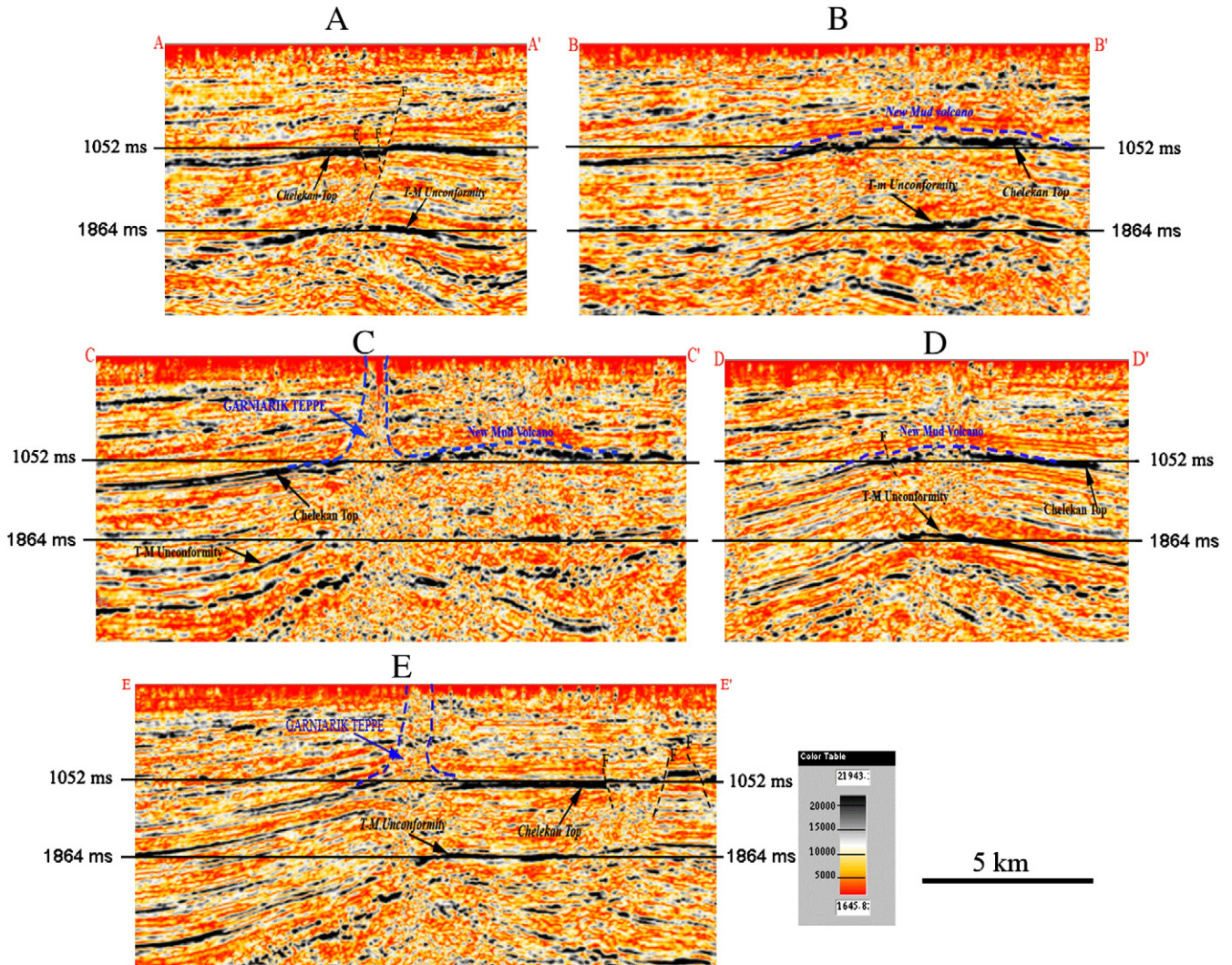


Fig. 5. The figures A to E are the vertical cross-sections of instantaneous amplitude attribute passing from Fig. 4 illustrating (the time line 1052 ms).

construction of Chelekan. Anticline structures in the coherence attribute usually appear as low coherence circular masses because of the least similarity between the traces (Marfurt and Duncan, 2002). Fig. 4 also illustrates a new mud volcano in the east part of the region as low coherence mass (black) in addition to GARNIARIK TEPE mud volcano (Rezvandehy, 2006) (these two-mud volcanoes are also seen

partially in Fig. 6). Vertical cross-sections D-D' and B-B' appear from the new mud volcano and the cross-section C-C' passes through both mud volcanoes. For further determining, their lengths have been drawn as blue dotted lines in vertical cross-sections and the faults also are shown as black dotted lines (Fig. 5). It is completely clear that the new mud volcano has not reached the surface and the GARNIARIK

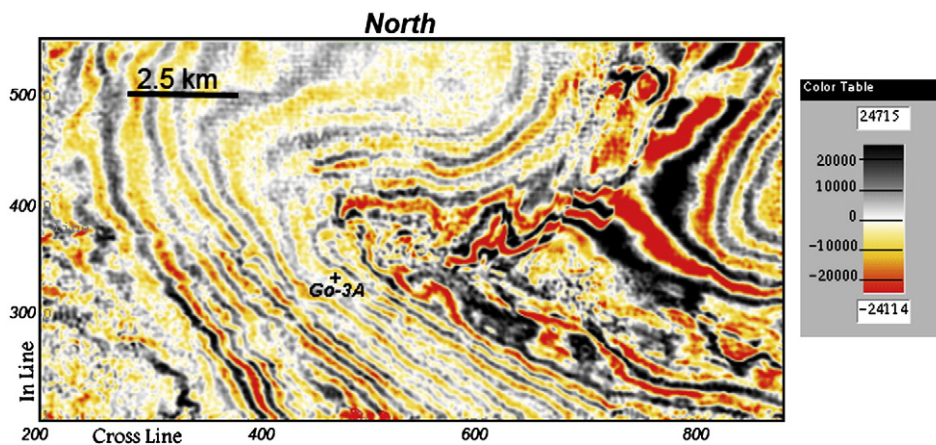


Fig. 6. Time slice at 1052 ms (Chelekan top at the well Go-3A).

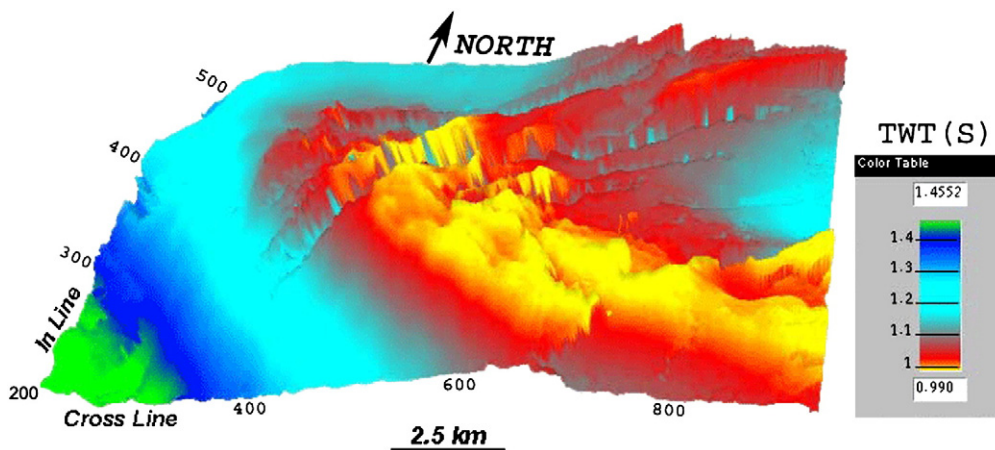


Fig. 7. Three dimensional time modeling of Chelekan top.

TEPPE mud volcano has penetrated into the ground. Furthermore, these two mud volcanos are connected beneath the ground (Rezvandehey, 2006).

Since there is an index seismic peak in Chelekan top (Fig. 5) this surface can be followed in the whole 3D seismic volume using instantaneous amplitude attribute and then model it as three dimensions with time dimension which is observed in Fig. 7. This figure illustrates the topography of the layers in Chelekan construction. Furthermore, most of the previously indicated faults can be observed in this figure.

4.2. Spectral decomposition attribute

Fig. 8 shows the frequency bands of 20, 30, 40 and 50 Hz of spectral decomposition attribute in Chelekan top (time slice 1052 ms) with time window of –200, 200 ms. High amplitude magnitude is shown as white and the low one in black. The exact horizontal formation of

GARNIARIK TEPPE mud volcano clearly observed in these frequency bands and it is only possible to model it through this attribute. The new mud volcano can be observed in the frequency bands in a complete limited way because the influencing area of this mud volcano is in a higher depth compared to the mud volcano of GARNIARIK TEPPE, and the frequency bands are chosen for showing the lateral vastness of GARNIARIK TEPPE mud volcano. For better determining the picture of the new mud volcano, the frequency bands 20, 30, 40 and 50 Hz are drawn in a higher time slice (1864 ms) with time window of –200, 200 ms, which can be seen in Fig. 9 and for a better observation, line time 1864 ms in Fig. 5. The new horizontal formation of this mud volcano in a complete way is apparent in these frequency bands. The high amplitude magnitude and the lateral vastness could be a sign of high gas potentials in this mud volcano. In all frequency slices, the high amplitude in the vicinity of mud volcanos can signify gas accumulation in order to hit an upper impermeable silty and clay layer, and in the center of that, gas can easily move

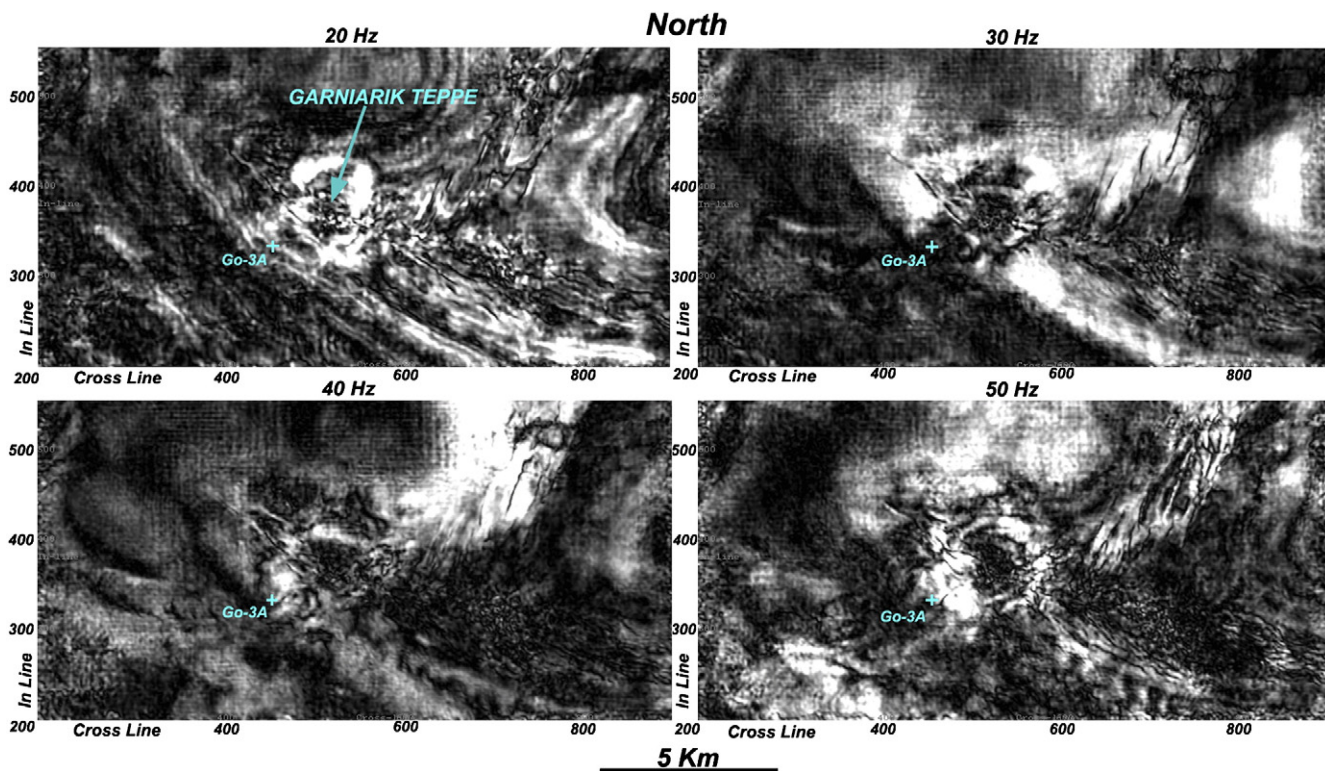


Fig. 8. The frequency bands 20, 30, 40 and 50 Hz of spectral decomposition attribute with the time window –200, 200 ms in the time horizon of Chelekan top (1052 ms).

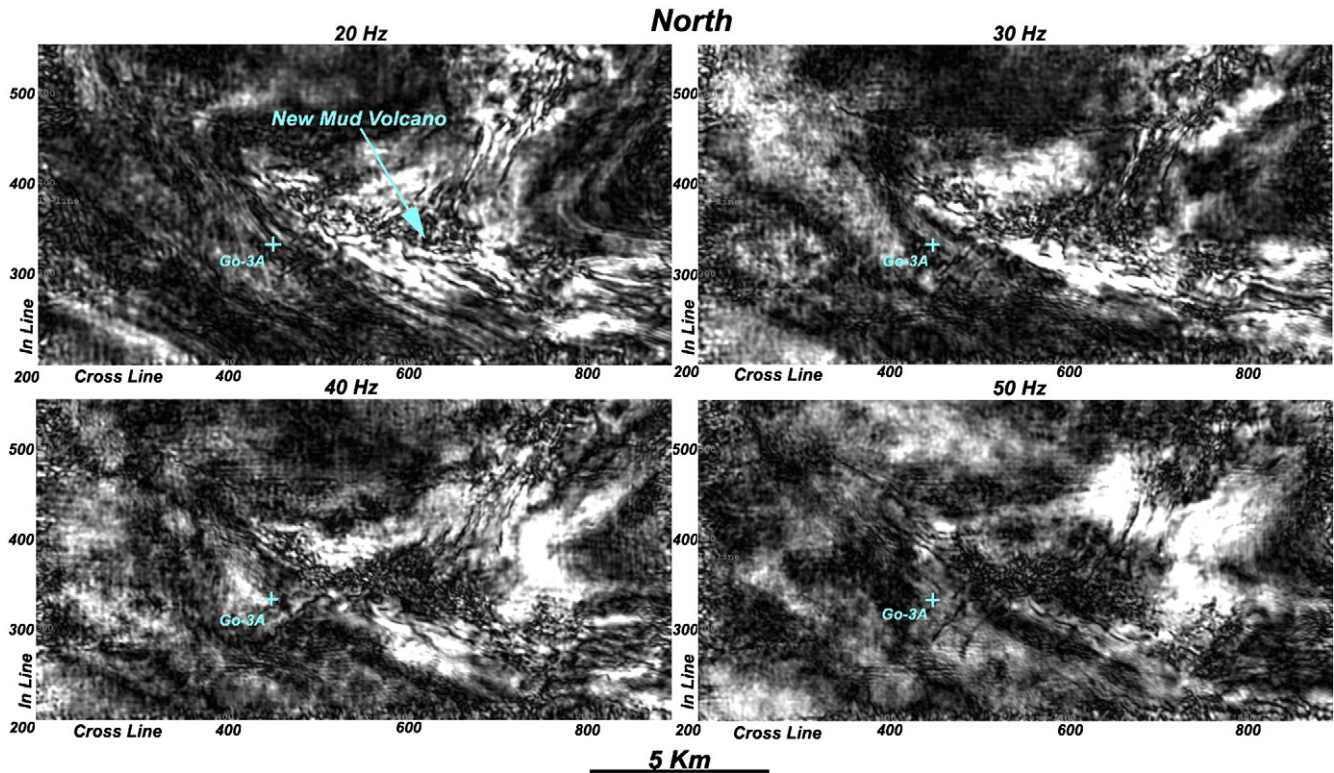


Fig. 9. The frequency bands 20, 30, 40 and 50 Hz of spectral decomposition attribute with the time window $-200, 200$ ms in the time horizon 1864 ms.

upward due to existence of loose clay layers, so the low amplitude is observed (Rezvandehy, 2006). This case is obvious in vertical slices of instantaneous amplitude in Fig. 5.

5. Modeling of gas layer

5.1. Construction of synthetic seismogram of well Go-3A and studying its results

Fig. 10 illustrates the computed impedance (using sonic and density logs) and synthetic seismogram in the well Go-3A. The synthetic seismogram resulted as a correlation over 68% with real seismic data. In this figure, it is completely clear that the gas sand layer contains very low impedance compared to the upper layers. However, even with this high impedance difference, no significant seismic peak is observed in the seismogram diagram. By calculating the critical resolution thickness index for this layer, which equals $1/8$ of the central frequency wavelength in the wave figure ($\lambda/8 = V/8f$) (Widess, 1973), the thickness of the gas layer (9.6 m) was less than the critical resolution thickness achieved (14.2 m). Therefore, it was impossible to estimate the thickness of this layer in the 3D seismic volume. In such a situation, the seismic reflections from the top and bottom of this layer form one reflector whose amplitude resulted from this mixed reflector gradually reduces inclining zero with a decrease of the layer thickness followed by the destructive effect of the reflectors (Neidell and Poggiagliolmi, 1977). The mentioned case can be considered as an improbability of observing of the bright spot phenomenon that resulted from gas layers. In Fig. 10, it is completely clear that the clay and silt layers in spite of having the acoustic impedance difference less than the gas layer with upper layers, show a very big seismic peak in synthetic seismogram the reason of which has high thickness (about 31 m). Due to being placed in watery and sand construction of Chelekan, high acoustic impedance difference is observed in this non-porous, compact clay and silt layers. Fig. 11 illustrates the horizontal time cross-section (1584 ms) and vertical instantaneous amplitude attribute a passing through the gas layer in

the well Go-3A. The gas layer as it was expected is observed as having low amplitude (without considering the check shot error) in the vertical and horizontal cross-section and the clay and silt layers are seen as high amplitude. The alignment of clay and silt layers in the vertical and horizontal cross-sections of Fig. 11 has been shown with blue dotted lines. Fig. 12 shows W-E vertical cross section of instantaneous amplitude passing through the well Go-3A. It is clear that the gas layer has low amplitude and Chelekan top, and the clay and silty layer have the highest amplitude. New mud volcano has been revealed in this figure, which has not reached the earth.

5.2. Determining the increase of the gas layer thickness in the 3D seismic volume

As mentioned before, it is impossible to estimate the thickness on the basis of passing time from this layer in seismic cross section due to the gas layer's less thickness, however, considering the increase of seismic amplitude with an increase of the layer thickness, the thickness can be determined by increasing the amplitude in seismic cross-section. Owing to not existing a suitable seismic pick for gas layer, so a tuning curve and critical resolution thickness of Chelekan top, which has noticeable seismic pick, were computed in order to exemplify how increasing the amplitude signifies increasing thickness (Fig. 13). We can approximately relate this figure to the gas layer because this layer is located in Chelekan formation. It is obvious that the temporal thickness in critical resolution thickness is constant when the real thickness is dwindling and the amplitude grows with increasing thickness until tuning thickness reaches the maximum amplitude and then decreases.

Also the increase of amplitude can be a sign of high acoustic impedance and the existence of reservoir of higher quality. In addition, owing to the small seismic peak of this layer (Figs. 10, 11, and 12) it is impossible to follow it in the seismic volume and map the amplitude magnitude as well. For this purpose, the instantaneous amplitude attribute on reflection of the gas layer is first calculated in synthetic seismogram, the gas layer is detected by one pick, actually

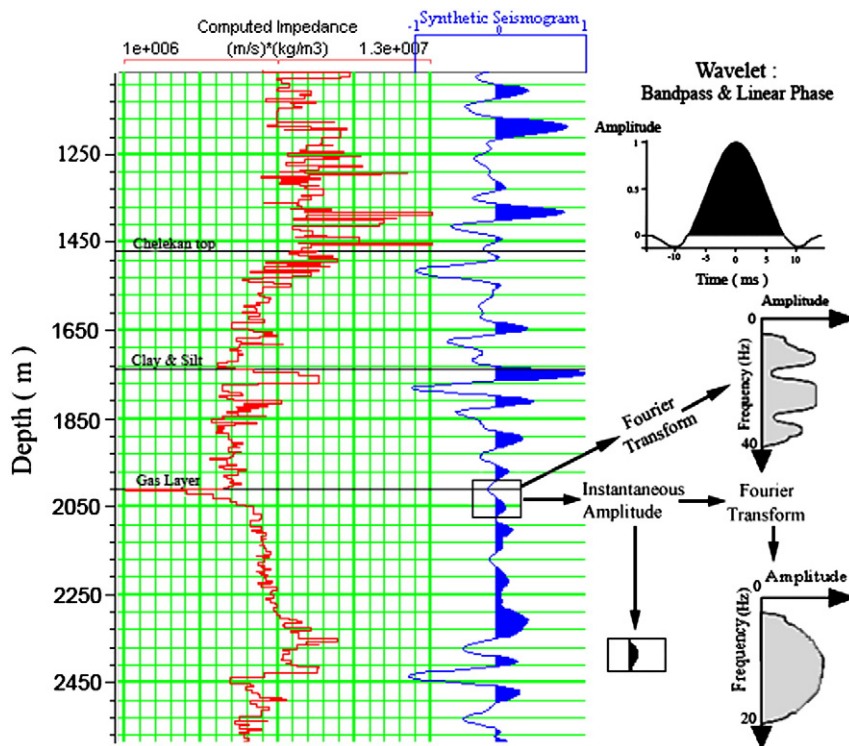


Fig. 10. The diagram of the computed impedance (red diagram, left side) and synthetic seismogram (blue diagram, right side) in the well Go-3A and bandpass wavelet with linear phase and Fourier Transform of synthetic seismogram of gas layer before and after computing instantaneous amplitude.

the negative amounts are eliminated so computing the dominant frequency will be more comfortable. Fig. 14 indicates instantaneous amplitude attribute of synthetic seismogram in the left one. As can be seen, gas layer like any other layers appears in the form of one single trace. This figure can be compared to Fig. 12, which shows the vertical cross section of instantaneous amplitude passing through the well Go-3A. Then, Fourier Transform of instantaneous amplitude related to the gas layer is achieved. In this way, the frequency related to the highest amplitude magnitude (dominant frequency) is chosen (Fig. 10). The frequency achieved was 9 Hz (Rezvandehy, 2006). It is completely apparent in Fig. 10 that it is more straightforward to opt for accurate dominant frequency with computing instantaneous amplitude, because there is a unique amplitude pick so following

this layer (after using instantaneous amplitude) would be easier in the whole 3D seismic volume.

For the final thickness modeling, first instantaneous amplitude attribute is calculated in the whole 3D seismic volume then the amount of the spectral decomposition attribute resulted from the output amplitude with the frequency of 9 Hz in time window of -200, 200 ms on time slice of the gas layer in the well Go-3A (1584 ms) is obtained, which is shown in Fig. 15 (Rezvandehy, 2006). The high amplitude is indicated in white and the low one in black. In fact, this map exactly shows the seismic amplitude changes of the gas layer in the whole 3D seismic volume. The high amplitude levels signify the higher thickness of the gas layer, which exist in the well Go-3A. Also, high amplitude is a sign of gas accumulation in this

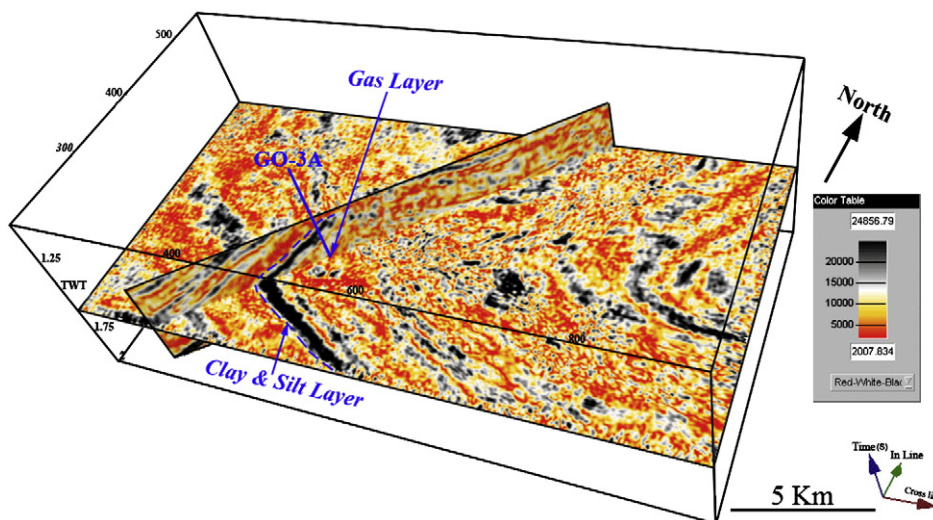


Fig. 11. The horizontal time cross-section (1584 ms) and the vertical instantaneous amplitude attribute passing through the gas layer in the well Go-3A. The alignment of clay and silt layers has been shown in blue dotted lines.

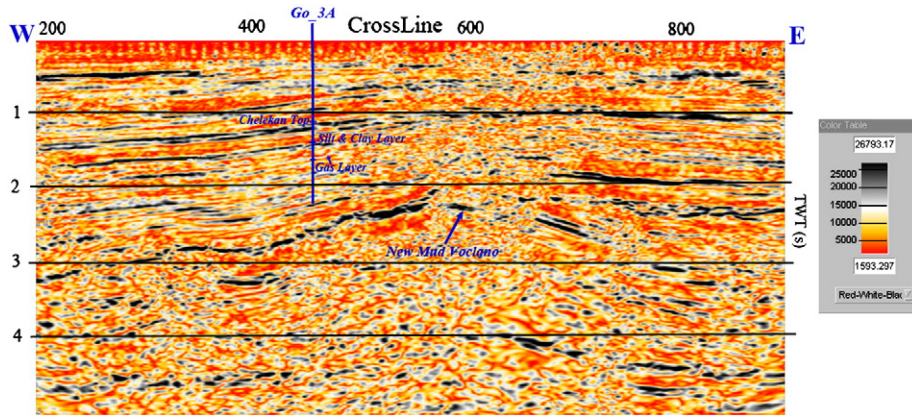


Fig. 12. W-E vertical cross section of instantaneous amplitude passing through the well Go-3A. The gas layer has low amplitude and Chelekan top and clay and silty layer have the highest amplitude. Also, new mud volcano has been marked in this figure.

reservoir, because this area (high amplitude) is a gas trap, which is faced to an upper impermeable and compact clay and silty layer and cannot escape toward low depth. Fig. 15 shows clearly that the gas reservoir has laterally been surrounded by this upper silty and clay layer.

5.3. Estimation of the least gas storage of the reservoir

To determine the least gas storage of this reservoir, the area of the blue dotted line is first calculated in Fig. 15 which is approximately $1.8 \cdot 10^7 \text{ m}^2$ (Rezvandehy, 2006). This area was calculated on the basis of the overall shape of the reservoir in Fig. 7 after conversion time to depth of this surface, although, the lateral expansion of the reservoir would be more than this region. In order to calculate the least gas storage, only the area of the high amplitude is calculated. Now the area achieved in the least gas layer thickness which is relevant to the thickness observed of the well Go-3A (9.6 m) is multiplied. Considering the fact that the region mentioned definitely has a thickness of more than 9.6 m (because the amplitudes obtained is higher) (Fig. 13) therefore it could be considered that the least volume of the gas layer is $1.6 \cdot 10^8 \text{ m}^3$. As a result, for determining the least gas storage, the

volume obtained is multiplied by the average porosity of the gas layer in the well Go-3A which equals 0.46. Therefore, the amount of this porosity is the least amount of the high amplitude region (an increase of the amplitude can be likely a rise sign of the acoustic impedance

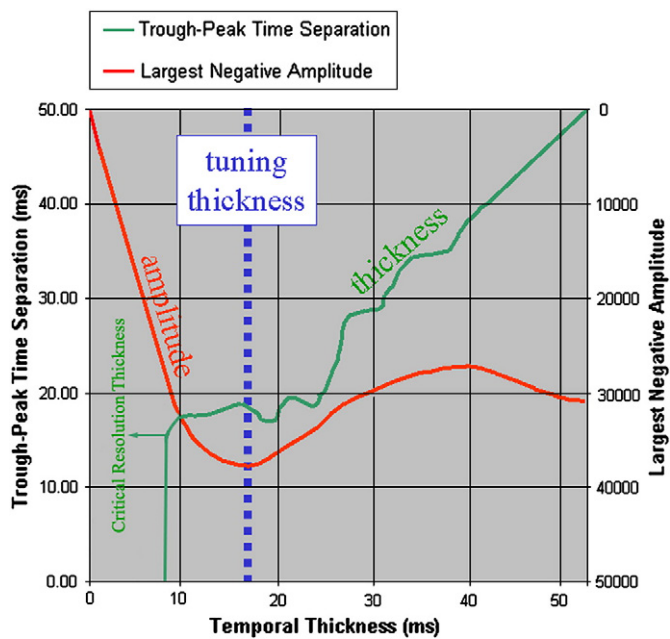


Fig. 13. Tuning curve and critical resolution thickness of Chelekan top.

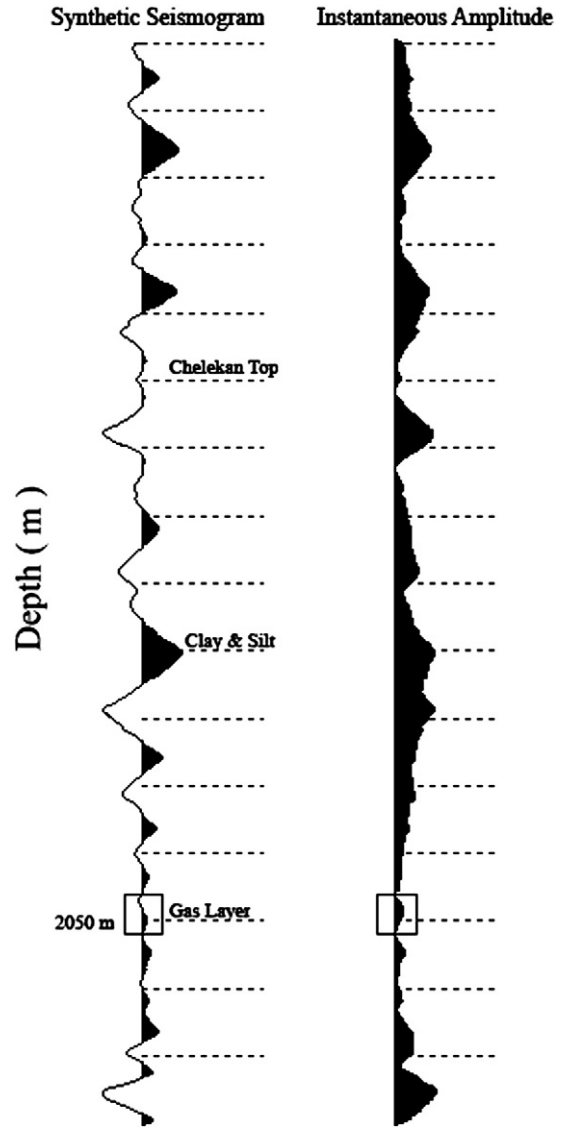


Fig. 14. Instantaneous amplitude attribute of synthetic seismogram.

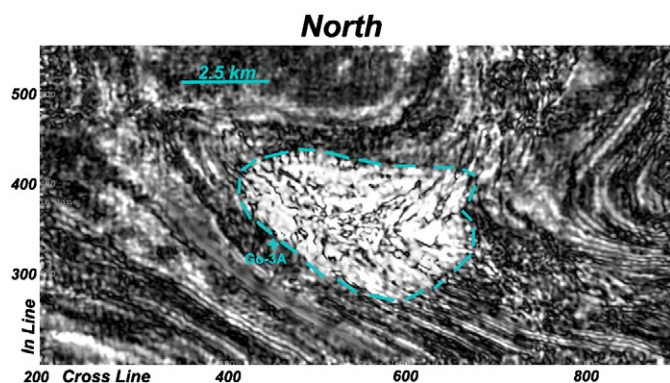


Fig. 15. The frequency band 9 Hz of spectral decomposition attribute in time window $-200, 200$ ms and the time horizon of gas layer in the well Go-3A (1584 ms). The blue dotted line region shows the increase of the thickness in the gas layer equal or more than the thickness observed in the well Go-3A (based on the amplitude magnitudes).

and following it is its porosity) so the least and obtainable gas storage of this reservoir equals $7.6 \cdot 10^7 \text{ m}^3$. It must be noted that regarding the existing huge amount of gas fields in the Southern part of Iran, this reservoir would not be economical to extract (Rezvandehy, 2006).

6. Conclusions

The simultaneous implementation of coherence, spectral decomposition, and instantaneous attributes in the geological modeling provided an acceptable answer and showed that although it seemed GARNIARIK TEPPE mud volcano was solely the cause of the gas potential of the well Go-3A, there was another deep mud volcano which has not reached the surface. This characteristic can be a sign that there is little gas potential unloading in this mud volcano, and considering the fact that its lateral vastness was also determined to be more than GARNIARIK TEPPE mud volcano, probably it has more gas potential compared to the GARNIARIK TEPPE mud volcano. These two mud volcanos are connected beneath the ground. The existence of two series of faults perpendicular to each other shows the sign of existence of tectonic pressures with the directions north eastern–south western and north western–south eastern following the formations of mud volcanos and are the main cause of the formation of the topography in the reservoir surface. The new method of integrating the instantaneous amplitude and spectral decomposition attributes clearly determined the accurate region where the thickness of the reservoir was increased. With regard to modeling mud volcanos and determining their lateral expansion it was determined that the existing gas in the increased region of the gas layer thickness was the result of mixing the gas potential of both mud volcanos of the reservoir which

had more inclination toward the new mud volcano. Because of the existence of loose and soft layers especially clay in mud volcanos, the gas can easily move upward, but whenever it contacts to an upper compact clay and silty layer, the gas is captured and forms this reservoir with high amplitude that is topographically more likely a closed anticline. The estimation of the gas layer was carried out approximately with the least available information. Although, the overall estimation of the amount of the existing gas in the reservoir was stated only with one well and the seismic data, the location of the best well points dug in the future for the most extraction of the gas could be predicted.

Acknowledgement

The authors would like to thank the National Iranian Oil Company (N.I.O.C), Exploration Directorate, for providing adequate data, and the detailed geological background of the reservoir and Mr. Behrank Kushavand from Alberta University for his useful peer review of the paper. We also would like to thank and appreciate Dr. Paul de Groot the president of dGB Earth Sciences and Dr. S. Hossein Hashemi the professor of Geophysics Institute of Tehran University for their guides in the implementation of opendtect software.

References

- Bahorich, M.S., Farmer, S.L., 1995. 3D seismic coherence for faults and stratigraphic feature. *The Leading Edge* 14, 1053–1058.
- Bahorich, M., Motsch, A., Loughlin, K., Partyka, G., 2002. Amplitude Responses Image Reservoir: Stratigraphic Imaging, *Seismic Advances*, pp. 59–61.
- Bracewell, R.N., 1965. *The Fourier Transform and Its Applications*. McGraw-Hill Book Co.
- Gersztenkorn, A., Shap, J., Marfurt, K., 1999. Eigenstructure based coherence computations as an aid to 3-D structural and stratigraphic mapping. *Geophysics* 64, 1468–1479.
- Hall, M., Trouillot, E., 2004. Predicting Stratigraphy with Spectral Decomposition. CSEG National Convention, Landmark Graphics, Calgary, Canada.
- K. Marfurt, W.S. Duncan, *Comparison of 3-D edge Detection Seismic Attributes to Vinton Dome Louisiana*, Allied Geophysical Laboratories, university of Houston; Paul Constance, output Exploration Co., Inc 2002, pp.1150–1165.
- Marfurt, K.G., Kirlin, R.L., Farmer, S.L., Bahorich, M.S., 1998. 3D seismic attributes using a running window semblance-based algorithm. *Geophysics* 63, 1150–1165.
- Neidell, N.S., Poggiagliolmi, E., 1977. In: Rayton, Charles E. (Ed.), *Stratigraphic Modeling and Interpretation Geophysical Principle and Techniques: Seismic Stratigraphy-Application to Hydrocarbon*. AAPG, Tulsa, Oklahoma, USA.
- Partyka, G., Gridley, J., Lopez, J., 1999. Interpretational application of spectral decomposition in reservoir characterization. *The Leading Edge* 18, 353–360.
- Rezvandehy, M., *Integrating seismic attributes in the accurate modeling of geological structures and determining the storage of the gas reservoir in Gorgan Plain*, Master of Science Thesis, Sahand University of Technology, Tabriz Iran, 2006.
- Taner, M.T., Sheriff, R.E., 1977. Application of amplitude, frequency, and other attributes to stratigraphic and hydrocarbon determination, *American Association of Petroleum Geologists. Memoir* 26, 301–327.
- Taner, M.T., 2000. *Attributes Revisited*, Rock Solid Images, Houston, Texas. <http://www.rocksolidimages.com>.
- Widess, M.B., 1973. How thin is a thin bed? *Geophysics* 38, 1176–1180.